STUDY OF BI-ORTHOGONAL MODES IN MAGNETIC BUTTERFLIES

PABLO D. MININNI[1], MARCELO LÓPEZ FUENTES[2], CRISTINA H. MANDRINI[3] and DANIEL O. GÓMEZ[1,3]

[1]*Departamento de Física, Facultad de Ciencias Exactas, Universidad de Buenos Aires, Ciudad Universitaria, 1428 Buenos Aires, Argentina (e-mail: dgomez@df.uba.ar)*

[2]*Naval Research Laboratory, Washington, DC 20375-5352, U.S.A.*

[3]*Instituto de Astronomía y Física del Espacio, Ciudad Universitaria, 1428 Buenos Aires, Argentina*

(Received 20 October 2003; accepted 19 November 2003)

Abstract. We present a bi-orthogonal decomposition of the temporal and latitudinal distribution of solar magnetic fields from synoptic magnetograms. Results are compared with a similar decomposition of the distribution of sunspots since 1874. We show that the butterfly diagrams can be interpreted as the result of approximately constant amplitudes and phases of two oscillations with periods close to 22 years. A clear periodicity of 7 years can also be identified in the most energetic modes of both spatio-temporal series. These results can be used to obtain relevant information concerning the physics of the solar dynamo.

1. Introduction

One of the most impressive features in solar physics is the cyclic behavior of the Sun. The number of sunspots varies with a period close to 11 years. The record of sunspot numbers is the only data set related to the solar magnetic field that reaches back to 1700, and is one of the longest and oldest systematic records in the history of astronomy. However, it was not until 1843 that the 11-year cycle was discovered (Schwabe, 1843). Five years later, Wolf introduced the modern criteria used to measure the sunspot number, and the amount of information on the solar cycle grew steadily since then.

The observational discoveries of Hale's law (Hale, 1908) and the reversal of the polar magnetic field (Babcock, 1961), led to the conclusion that the sunspot cycle is just one of the outcomes of the roughly periodic behavior of the Sun's magnetic field, with a mean period of 22 years. This magnetic field observed at the solar surface is believed to be produced by a dynamo process operating in the solar interior. According to dynamo theories, the number of sunspots and its spatial distribution are in phase with the strong toroidal magnetic field in the solar interior (Stix, 1976), nowadays believed to be located at the base of the convective region. Both linear (Hoyng, 1993) and nonlinear models (Dikpati and Charbonneau, 1999; Mininni and Gómez, 2002) are used to explain the observed dynamics. Although current dynamo models are able to explain the periodic behavior of solar magnetic fields, their agreement with observations relies on assumptions which are

Solar Physics **219:** 367–378, 2004.

not clearly understood, such as those invoked by mean field (Krause and Radler, 1980) or Babcock–Leighton dynamos (Dikpati and Charbonneau, 1999). Other hypotheses, such as the location of the source of poloidal field, are still a matter of debate (Nordlund *et al.*, 1992). Recently, it has been shown that Babcock–Leighton models with a source term near the surface lead to solutions with the wrong equatorial symmetry (Dikpati and Gilman, 2001). Also, the nature of the mechanism responsible for the saturation of the dynamo is ill understood, and several models exist using different mechanisms.

A closer inspection of the sunspot time series shows that it is not exactly periodic, displaying fluctuations both in its frequency and in the extent and intensity of its maxima. The sunspot number varies as much as 100% from cycle to cycle, while the period displays fluctuations within the range from 9 to 13 years. The origin of these irregularities is still unclear, and has become one of the most actively debated problems in solar physics. While dynamo models explain the mean properties of the solar cycle reasonably well, the nature of the irregularities remains essentially unknown. Broadly speaking, two rather different mechanisms have been invoked in the literature to account for these irregularities: chaos and stochasticity. In the chaotic scenario, the equations give a deterministic rule of evolution with complex dynamics (Zeldovich, Ruzmaikin, and Sokoloff, 1983; Knobloch and Landsberg, 1995). As an alternative approach, the scenario of a stochastically driven solar dynamo has been studied in a number of papers (Choudhuri, 1992; Hoyng, 1993). In these models, the random forcing is the end result of the stochasticity underlying the magnetic eruption which generates the spots. It is of course important to determine what types of mechanisms are responsible for the observed complexity, especially because several qualitative aspects of the system seem to be reproduced with either stochastic or deterministic approaches. Searches for signatures of a low-dimensional chaotic attractor in the sunspot time series are not conclusive, due to insufficient number of data (Carbonell, Oliver, and Ballester, 1994). Also, recent studies have shown that the standard algorithms used to search for signatures of a low-dimensional chaotic attractor in time series can lead to spurious convergence when applied to limited time-series (Paluš and Novotná, 2002). However, little effort has been done on the analysis of the spatio-temporal data. In a recent paper (Mininni, Gómez, and Mindlin, 2002), a first analysis of the bi-orthogonal decomposition (BOD) of the latitudinal and temporal distribution of the sunspots was made. The results obtained proved useful to make quantitative comparisons with theoretical models. Also, a detailed analysis of these results showed that the irregularities in the solar cycle are the result of the superposition of two constant amplitude and phase oscillations on a stochastic background, and are not a manifestation of low-dimensional chaos. It seems apparent that BOD studies yield valuable information on the physical mechanisms acting on the solar cycle, which can in turn be essential to address some of the open questions in the field.

In order to relate sunspot data with magnetic fields, some hypotheses are required. Therefore, in the present work we extend the previous analysis to the

latitudinal and temporal distribution of magnetic fields from solar magnetograms. The spatio-temporal distribution of sunspots (Gokhale *et al.*, 1992) or magnetic fields (Stenflo and Voguel, 1986) have so far been used to search for dispersion relations, but not to characterize the complexity of these datasets. Also, in spite of the limited time span covered by magnetograms, previous decompositions (Stenflo and Voguel, 1986; Gokhale *et al.*, 1992) have been carried out using Fourier or spherical harmonic expansions. The bi-orthogonal decomposition has the major advantage of being linearly optimal, since modes are ordered by their energies rather than by their wave numbers. This property facilitates the identification of the most important modes for the dynamics. Relevant information concerning periodicities and nonlinearities is obtained from the analysis of the decomposition. Also, the results are in good agreement with the results presented in Mininni, Gómez, and Mindlin (2002), and therefore bring a strong confidence to our previous results and to the stochastic scenario. In Section 2 we present the different sets used to perform the analysis. In Section 3 we make a brief description of the statistical tool used to decompose the data. Section 4 shows the results obtained and Section 5 lists the main conclusions of this work.

2. The Data

To compute a bi-orthogonal decomposition of the latitudinal and temporal distribution of magnetic fields (dataset M), we have used synoptic maps obtained by the National Solar Observatory at Kitt Peak (NSO/KP) (see *ftp://argo.tuc.noao.edu/kpvt/synoptic/README*). The maps consist of rectangular arrays built from daily full-disk line-of-sight magnetograms using a triangular weighted integration. The result of this procedure is arranged in an array from right to left (west to east) as time evolves. The arrays have a 360×180 pixels format. Each pixel in the horizontal direction corresponds to a heliographic longitude of 1°, while in the vertical direction they correspond to the sinus of the latitude in heliographic coordinates. Therefore, each map corresponds to a time span of one Carrington rotation. Each pixel contains the time and space averaged magnetic flux per unit surface crossing the photosphere at a given position on the Sun. Projection effects are taken into account by correcting the flux according to the real solar area covered by a particular pixel and by assuming that the photospheric field is radial. Figure 1 shows a magnetic field butterfly built by averaging in longitude (at each latitude) all the synoptic maps from June 1975 to December 2000. The averaged magnetic field values are arranged in a rectangular array in which the horizontal direction corresponds to time and the vertical direction to the sinus of the latitude.

To obtain information of long temporal trends, we also used the Wolf number data as measured by the Royal Greenwich Observatory (RGO), starting in May 1874 (dataset W). Although this observatory discontinued the data set in 1976, the Solar Optical Observing Network (SOON) and the US National Oceanic and

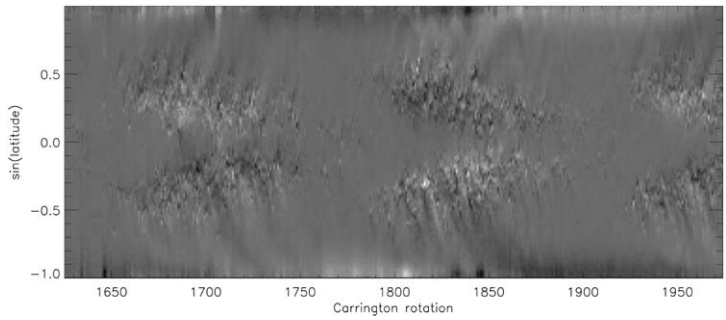

Figure 1. Magnetic butterfly obtained from Kit Peak synoptic maps (dataset M).

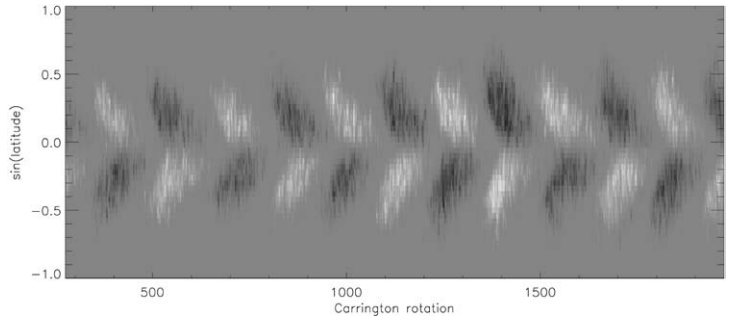

Figure 2. Inferred magnetic butterfly from sunspot data (dataset W).

Atmospheric Administration (NOAA) continued compiling the data in a format consistent with RGO standards. Hereafter we will regard this set of data as the RGO data set. This data set includes not only the information of number of sunspots, but also of their sizes and position on the solar disc. The data plotted in the butterfly diagram is the result of computing the area covered by sunspots in strips of constant projected area aligned in latitude. In order to build a spatio-temporal series able to serve as a proxy of the toroidal magnetic field (see Figure 2), the sunspot data were processed to explicitly show magnetic field reversals (Mininni, Gómez, and Mindlin, 2002). A similar process to obtain a proxy of magnetic fields from sunspot data has been previously used by Gokhale *et al.* (1992).

Several features of these butterfly diagrams are striking: the absence of sunspots at high latitudes, and the equator-ward drift of the sunspot distribution as the cycle evolves. Note that the latitudinal distribution of sunspots is not exactly periodic, and that north–south asymmetries can also be identified. At solar minima, spots from the new cycle are born at mid-latitudes, while spots from the preceding cycle are still present near the equator.

Note that although both datasets provide information concerning the cycle of solar activity, they are obtained with rather different instruments and techniques and are quite independent from one another. On one hand, the data obtained from solar magnetograms yield information about the complete spatial distribution of

magnetic fields with a relatively short time span (only one complete magnetic cycle). On the other hand, the sunspot areas provide information about the latitudes where sunspots are observed, with a much longer time span.

3. Bi-orthogonal Decomposition

The bi-orthogonal decomposition (BOD) was independently proposed by Kosambi (1943), Loève (1945), and Karhunen (1946) as an appropriate space–time decomposition of regular and complex phenomena. This tool consists of decomposing a spatio-temporal signal into an orthogonal set of temporal and spatial modes, with a view to extracting dominant features and trends from the dataset. These empirical modes are in general coupled to one another, and are eigenvectors of a linear operator obtained from the data. The BOD has been used to study different phenomena in several disciplines, such as image processing (Rosenfeld and Kak, 1982), data compression (Andrews, Davies, and Schwartz, 1967), signal analysis (Algazi and Sakrison, 1969), random variables (Papoulis, 1965) or oceanography (Preisendorfer, 1988). To our knowledge, it has been applied to astrophysical datasets only very recently (Carbone *et al.*, 2002; Mininni, Gómez, and Mindlin, 2002).

One of the most interesting features of this decomposition is optimality, in the sense that it provides the most efficient way of capturing the dominant components of infinite-dimensional processes with only a few modes. This optimality results from the fact that the empirical modes are ordered by their energies rather than by their wavenumbers (Holmes, Lumley, and Berkooz, 1996). When applied to turbulent flows, the BOD provides a representation for the mean and fluctuating velocity fields, and the corresponding modes can be related to two-point velocity correlations (Pope, 2000). In this sense, the modes that we obtain yield relevant information for closures of the dynamo equation.

Given a spatio-temporal (and in general complex valued) signal $u(x, t)$, where $x \in X$ and $t \in T$ are respectively the space and time variables, we can define a linear operator $U : H(X) \to H(T)$ such that

$$\forall \phi \in H(X) \quad (U\phi)(t) = \int_X u(x, t)\phi(x)\, \mathrm{d}x \ , \tag{1}$$

where H is a linear Hilbert space with the standard inner product. The adjoint operator $U^* : H(T) \to H(X)$ is given by

$$\forall \psi \in H(T) \quad (U^*\psi)(x) = \int_T \overline{u(x, t)}\psi(t)\, \mathrm{d}t \ , \tag{2}$$

where the overbar denotes a complex conjugate operation. Assuming that U is a compact operator, its spectrum consists of a denumerable set of singular points and the signal $u(x, t)$ can be written as

$$u(x,t) = \sum_{k=1}^{\infty} \alpha_k \overline{\phi_k(x)} \psi_k(t) \ , \tag{3}$$

where α_k, ϕ_k and ψ_k are elements of the spectral decomposition of the operator U. More specifically, they are solutions of the eigenvalue problem given by

$$(U^* U \phi_k)(x) = \alpha_k^2 \phi_k(x), \tag{4}$$

$$(U U^* \psi_k)(t) = \alpha_k^2 \psi_k(t). \tag{5}$$

The square values of the eigenvalues $\alpha_k, k = 1, \ldots, \infty$ are known as the '*energies*' of the corresponding modes and satisfy the conditions $\alpha_1 \geq \alpha_2 \geq \cdots > 0$, $\lim_{k\to\infty} \alpha_k = 0$. The spatial eigenfunctions $\phi_k, k = 1, \ldots, \infty$ are termed '*topos*' and are mutually orthogonal, i.e. $(\phi_k, \phi_l) = \delta_{k,l}$. In turn, the temporal eigenfunctions $\psi_k, k = 1, \ldots, \infty$ are known as '*chronos*', and also satisfy the orthogonality conditions $(\psi_k, \psi_l) = \delta_{k,l}$. The series of Equation (3) is convergent in norm.

The series shown in Equation (3) represents the BOD of the signal $u(x,t)$. Two particular examples of this decomposition are the well known two dimensional Fourier decomposition and the proper orthogonal decomposition used in probability theory (Holmes, Lumley, and Berkooz, 1996). Let us assume that the matrix U_{ij} $(i = 1, 2, 3, \ldots, N_X;\ j = 1, 2, 3, \ldots, N_T)$ stores the area of the sunspots for different latitudes and times. That is to say, i labels the N_X latitude bins and j labels the N_T Carrington rotations available in the data set (the same procedure is applied to the data from synoptic maps). In both datasets $N_T \gg N_X$. Then the matrix U^*U is computed, where the asterisk denotes transposed and conjugated matrix. Eigenvalues and eigenvectors of U^*U are obtained (note that this is a relatively small problem involving only a $N_X \times N_X$ matrix). From Equation (4) it follows that the eigenvalues obtained are the energies α_k^2 (here k labels the ordering, from larger to smaller), while the eigenvectors are the empirical modes denoted in the continuum case as $\phi_k(X)$. Therefore, for the discrete data set the topos are N_X vectors of N_X components each.

The chronos in Equation (5) could be obtained in the same way by solving the eigenvalue problem for the matrix UU^*. However, this is a larger matrix with $N_T \times N_T$ elements. Instead, Equation (1) can be used. Therefore, the N_X vectors with N_T elements representing the chronos are obtained after multiplying the row vectors of the topos with the matrix U, except for a normalization factor.

In summary, when dealing with a finite and discrete dataset, the sum in Equation (3) will run up to a finite number. Also, Equations (4) and (5) reduce to a spectral problem for the square matrices $UU^* \in N_T \times N_T$ and $U^*U \in N_X \times N_X$. For instance, the spatial eigenvectors of $U^*U \in N_X \times N_X$ can be interpreted as the principal axes of the cloud of data points $u(\mathbf{x}, t_j)$, $j = 1, \ldots, N_T$ in the N_X-dimensional vector space. Our goal in this paper is to perform the BOD of dataset M and compare it with results from dataset W, to extract useful information on the solar magnetic cycle.

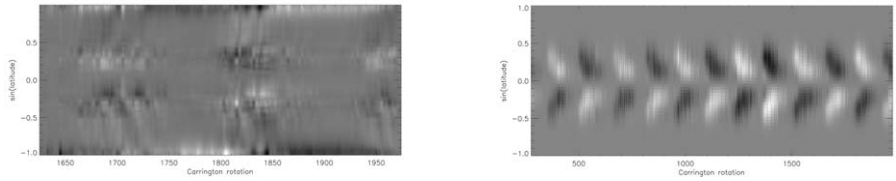

Figure 3. Reconstruction of datasets M and W.

4. Data Analysis

In Figure 3(a) we show butterfly patterns reconstructed using the first 5 modes of the bi-orthogonal decomposition of dataset M. These modes remarkably describe the mean properties of the solar cycle. Several features observed in the solar butterfly diagram can also be identified in this truncated version, such as the absence of sunspots at high latitudes, and the equator-ward drift of the sunspot distribution. These modes alone comprise the 80.6% of the total energy of the system, where the energy of each mode k is defined as the square of its amplitude α_k. On the other hand, the first two modes contain 63.24% of the total energy. However, when reconstructing the diagrams with the first two modes, the main features of the solar cycle can be still identified.

When considering dataset W, only the first two modes (with 84.4% of the energy) are needed to reconstruct the magnetic butterfly diagram (see Figure 3(b)). The BOD is a statistical tool, and as a result the quality of the decomposition is dependent on the length of the dataset. Therefore, the dispersion of the energy in several modes in case M can be expected since the dataset only covers one complete magnetic cycle.

The first topo of decomposition M has a strong component related with the dynamics of the magnetic fields at the poles (see Figure 4(a)). Its energy is about 45% of the total energy of the decomposition. Also, weaker features at intermediate latitudes can be identified. This strong polar intensity is not present in decomposition W, since this dataset provides no information about the dynamics near the poles. However, note that the intensity at the poles in dataset M is strongly enhanced during the process of building the butterfly diagram, as a result of the relatively weak fluctuations observed in the poles. Therefore, the mean value over a Carrington rotation strongly increases its energy. This can be verified when considering the absolute value of the magnetic fields, since in that case the intensity is much smaller. We therefore consider this strong distribution of magnetic fields in the polar regions as an artifact, and as a consequence will skip this mode when comparing with dataset W.

As previously discussed, topos from dataset W show no dynamics in the poles (Figure 4(b)). This is an expected result, since the data are related with the sunspot areas. However, out of the polar regions, topos 1 and 2 from dataset W coincide qualitatively with topos 2 and 3 from dataset M. Note that these are the modes

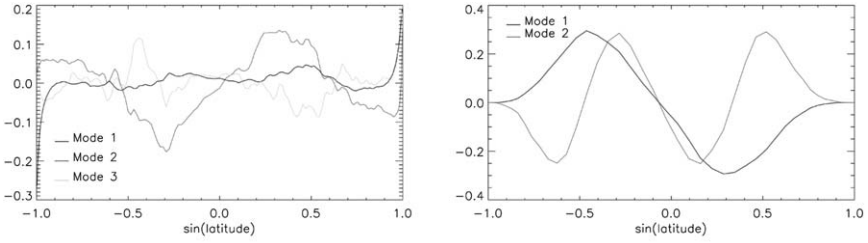

Figure 4. First topos for decompositions M and W.

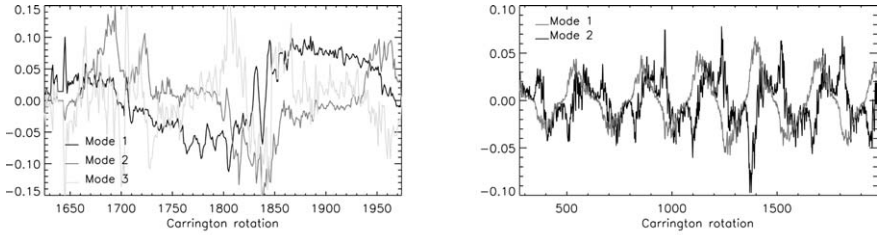

Figure 5. Chronos for decompositions M and W.

which correspond to activity at mid-latitudes, and can therefore be compared with information from dataset W. The chronos associated with these first topos (dataset M, see Figure 5(a)) show an almost constant phase shift. When one of the chronos is about to change sign, the other is near a maximum or minimum.

This behavior is also observed in dataset W (see Figure 5(b)), where we observe the two first topos to display a 22-year cycle and a constant phase shift. Therefore, the butterfly diagrams could be interpreted as the result of the approximately constant amplitudes and phases of two odd oscillations with periods close to 22 years. The alternation between the maxima of each mode gives rise to the migration of magnetic activity towards the equator and therefore to the butterfly diagrams. Here resides the major advantage of the bi-orthogonal decomposition: the modes are ordered by their energies rather than by their wave numbers, thus allowing the identification of the most important modes for the dynamics. The rest of the modes have amplitudes which are much smaller than these first two.

Figure 6 shows the power spectra of the chronos corresponding to the first modes of decomposition M. In these first modes, a periodicity close to 7 years can be seen, which has also been reported by Bracewell (1985) for the Wolf time series. As we discuss below, this periodicity suggests the presence of a nonlinear deterministic oscillation driving the first two modes. Apart from the power ridge in the frequency band close to 7 years, no other spectral features can be observed.

Essentially the same features (a strong peak near 22 years) can be identified in the spectra of the chronos corresponding to dataset W (see Figure 7). Also, a weak peak close to 4 years can be observed. The strong peak close to 7 years

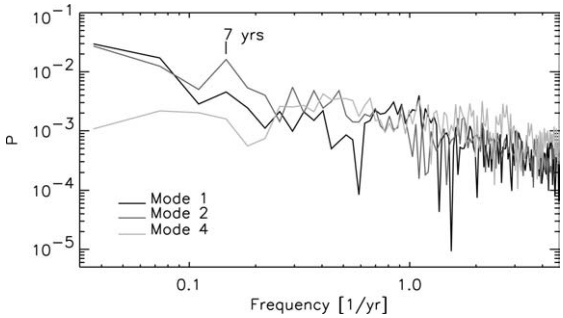

Figure 6. Spectrum of the chronos for decomposition M.

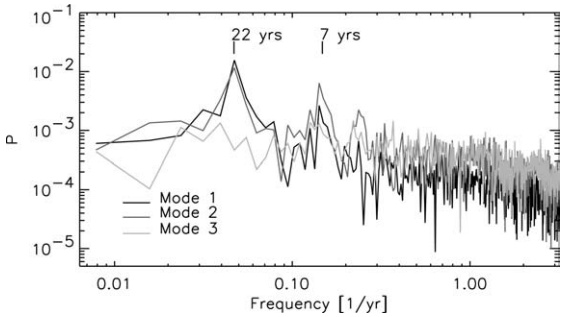

Figure 7. Spectrum of the time traces of decomposition W.

observed in both datasets gives strong confidence to this result. In a previous paper (Mininni, Gómez, and Mindlin, 2002), it was shown that this peak (and also the 4 years periodicity) can be generated from beating considering an odd nonlinearity in the deterministic equations governing the system (see also Landau, 1976). For instance, a cubic nonlinearity in the dynamo equations would cause that an initially harmonic solution with frequency ω (corresponding to a period of 22 years) develops a peak at a frequency 3ω (Bracewell, 1985; Mininni and Gómez, 2003). As a result, the initial harmonic solution develops an asymmetry in its time evolution, with a fast increase and a slow decay, as observed in the sunspot time series (Mininni, Gómez, and Mindlin, 2000). Note that these results are compatible with the commonly used expression for α-quenching (Dikpati and Charbonneau, 1999) of the form $\alpha(B) = \alpha_0 B/(1 + B^2) \approx \alpha_0(B - B^3)$.

The spectra corresponding to the remaining chronos show no clear features whatsoever. Moreover, autocorrelation tests for decomposition W suggest that it has no correlation at 22 years or at its harmonics, and therefore it seems to be just noise. For the chronos corresponding to the first two modes of both datasets (see Figures 8 and 9), the autocorrelation coefficients show positive correlation in the time lag equal to zero, and negative correlations in time lags approximately equal to ± 11 years. Modes 1 and 2 from dataset W also show positive correlation at time lags close to ± 22 years. On the other hand, the autocorrelation of the remaining

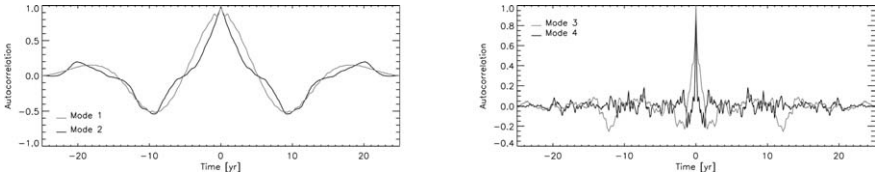

Figure 8. Auto-correlation for the first modes of decomposition M.

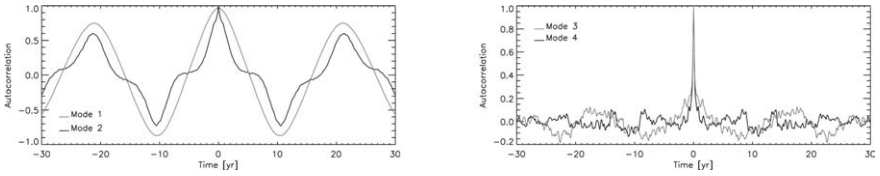

Figure 9. Auto-correlation for the first modes of decomposition W.

chronos fall immediately below 0.2, which implies a strong irregular component in these time series. This effect can be observed in both the spectra and autocorrelation coefficients of any of these chronos. Note that the first mode of dataset M also shows a strong periodicity of 1 year. This is a spurious effect caused by the rotation of the Earth. Since the magnetic axis of the Sun is not exactly perpendicular to the ecliptic, the projection of the poles contribution modulates the amplitude observed in the magnetograms.

In the decomposition of the magnetic butterflies (i.e., dataset M), 72.7% of the total energy is comprised in modes which are antisymmetric with respect to the equator. The first two modes contain 63.2% of the energy, and are antisymmetric. On the other hand, in the decomposition obtained from the sunspot area (dataset W), the first two modes contain 84.4% of the total energy, and all antisymmetric modes together retain 90.4% of the energy. Since the BOD is essentially a statistical decomposition, the bigger dispersion of the energy in the decomposition of the magnetic butterflies can be associated with the fact that only one cycle is available for the analysis. Therefore, the solar magnetic field shows a strong equatorial anti-symmetry, which also means that the sunspot distribution is nearly symmetric. Only a weak departure from this behavior have been measured in both datasets. Recently, it was shown that some Babcock–Leighton models tend to develop equatorially symmetric modes when the equations are solved in both hemispheres (Dikpati and Gilman, 2001). Therefore, the degree of deviation from this symmetry (or anti-symmetry) is another property that can be used to validate or refute theoretical models.

5. Discussion

We present a bi-orthogonal decomposition of the temporal and latitudinal distribution of solar magnetic field intensities derived from Kitt Peak magnetograms.

These results are compared with a similar decomposition of the distribution of sunspots areas collected by the Royal Greenwich Observatory since 1874. A clear periodicity of 7 years can be identified in the most energetic modes of both spatio-temporal series. Also, a strong periodicity at 22 years and a much weaker periodicity close to 4 years can be observed in the modes from the distribution of sunspots areas. The period of about 7 years is indicative of the presence of odd nonlinearities in the dynamo equations underlying the generation of magnetic field on the Sun. To our knowledge, the periodicity of 7 years was first reported by Bracewell (1985), who also interpreted this result as the consequence of a cubic nonlinearity.

Another important finding of the present study, is the fact that modes obtained from both datasets (i.e., magnetograms and sunspots) are qualitatively similar, and display the same spectral and autocorrelation features. This similarity, in turn, indicates that magnetograms and sunspots are indeed two observable outcomes of the same physical process. On one hand, dataset M contains the spatio-temporal distribution of a physical quantity such as the magnetic field intensity. However, its statistical quality is somewhat limited because of the (necessarily) small time coverage. On the other hand, the relationship of the sunspot area (contained in dataset W) with the underlying physical variables is more obscure. But since the time coverage is so much larger, it strengthens the statistical value of this dataset. Therefore, the above-mentioned similarity between both datasets brings a strong confidence to previous results (Mininni, Gómez, and Mindlin, 2002), which were obtained only from the sunspot area distribution. Analysis of these results shows that the irregularities observed in the solar cycle can be interpreted through a superposition of two antisymmetric modes interacting with a stochastic background. The information provided by the BOD can be used to validate models for the solar cycle, as well as to obtain information of symmetries and nonlinear effects. Also, truncated models can be derived by projecting the dynamical equations on the empirical modes (Holmes, Lumley, and Berkooz, 1996; Carbone *et al.*, 2002).

Acknowledgements

This research was supported by the University of Buenos Aires (grant X209/00). The authors also acknowledge partial support from the *Agencia Nacional de Promoción de Ciencia y Tecnología* (grant PICT 03-9483).

References

Algazi, V. R. and Sakrison, D. J.: 1969, *IEEE Trans. Inform. Theory* **15**, 319.
Andrews, C. A., Davies, J. M., and Schwartz, G. R.: 1967, *Proc. IEEE* **55**, 267.
Babcock, H. W.: 1961, *Astrophys. J.* **133**, 572.
Bracewell, R. N.: 1985, *Australian J. Phys.* **38**, 1009.
Carbone, V. and 10 co-authors: 2002, *Astron. Astrophys.* **381**, 265.

Carbonell, M., Oliver, R., and Ballester, J. L.: 1994, *Astron. Astrophys.* **290**, 983.
Choudhuri, A. R.: 1992, *Astron. Astrophys.* **253**, 277.
Dikpati, M. and Charbonneau, P.: 1999, *Astrophys. J.* **518**, 508.
Dikpati, M. and Gilman, P. A.: 2001, *Am. Soc. Pacific CS* **248**, 125.
Gokhale, M. H., Javaraiah, J., Kutty, K. N., and Varghese, B. A.: 1992, *Solar Phys.* **138**, 35.
Hale, G. E.: 1908, *Astrophys. J.* **28**, 315.
Holmes, P., Lumley, J. L., and Berkooz, G.: 1996, *Turbulence, Coherent Structures, Dynamical Systems and Symmetry*, Cambridge University Press, Cambridge.
Hoyng, P.: 1993, *Astron. Astrophys.* **272**, 321.
Karhunen, K.: 1946, *Ann. Acad. Sci. Fennicae* **A1**, 34.
Knobloch, E. and Landsberg, A. S.: 1995, *Monthly Notices Royal Astron. Soc.* **278**, 294.
Kosambi, D. D.: 1943, *J. Indian Math. Soc.* **7**, 76.
Krause, F. and Radler, K. H.: 1980, *Mean Field Magnetohydrodynamics and Dynamo Theory*, Pergamon, Oxford.
Landau, L. D. and Lifshitz, E. M.: 1976, *Mechanics*, 3rd ed., Pergamon, Oxford.
Loève, M.: 1945, *Comptes Rendus Acad. Sci. Paris* **1**, 220.
Mininni, P. D., Gómez, D. O., and Mindlin, G. B.: 2000, *Phys. Rev. Lett.* **85**, 5476.
Mininni, P. D., Gómez, D. O., and Mindlin, G. B.: 2002, *Phys. Rev. Lett.* **89**, 061101.
Mininni, P. D. and Gómez, D. O.: 2002, *Astrophys. J.* **573**, 474.
Mininni, P. D. and Gómez, D. O.: 2003, *Phys.* **A327**, 54.
Nordlund, A. and 6 co-authors: 1992, *Astrophys. J.* **392**, 647.
Paluš, M. and Novotná, D.: 1999, *Phys. Rev. Lett.* **83**, 3406.
Papoulis, A.: 1965, *Probability, Random Variables and Stochastic Processes*, McGraw-Hill, New York.
Pope, S. B.: 2000, *Turbulent Flows*, Cambridge University Press, Cambridge.
Preisendorfer, R. W.: 1988, *Principal Component Analysis in Meteorology and Oceanography*, Elsevier, Amsterdam.
Rosenfeld, A. and Kak, A. C.: 1982, *Digital Picture Processing*, Academic Press, New York.
Schwabe, S. H.: 1843, *Astron. Nachr.* **20**, 283.
Stenflo, J. O. and Vogel, M.: 1986, *Nature* **319**, 285.
Stix, M.: 1976, *Astron. Astrophys.* **47**, 243.
Zeldovich, Y. B., Ruzmaikin, A. A., and Sokoloff, D. D.: 1983, *Magnetic Fields in Astrophysics*, Gordon and Breach, New York.